AD-A151 301 HIGH CURRENT BEAM HOLLOWING INSTABILITY STUDY(U) 1/1
MISSION RESEARCH CORP ALBUQUERQUE NM C A EKDAHL JAN 85
AMRC-R-671

UNCLASSIFIED F/G 20/8 NL

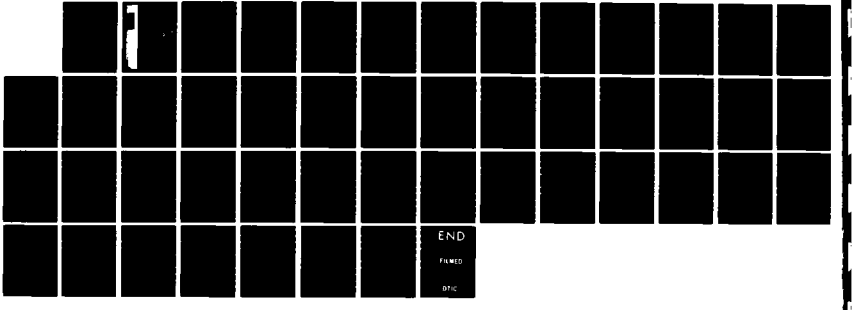

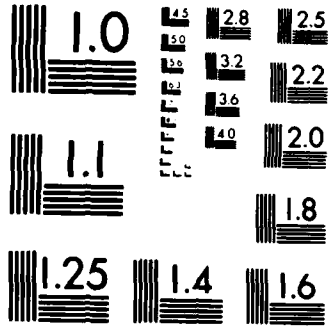

MICROCOPY RESOLUTION TEST CHART
NATIONAL BUREAU OF STANDARDS-1963-A

AMRC-R-671
Copy

FINAL TECHNICAL REPORT

High Current Beam Hollowing Instability Study

Brendan B. Godfrey
Mark M. Campbell
Barry S. Newberger
Lawrence A. Wright

and

Carl A. Ekdahl (SNLA)

January 1985

Prepared for: Sandia National Laboratories
Pulse Power Directorate
Albuquerque, New Mexico 87195

Work Order: 48-1044 (17 August 1983)

Prepared by: MISSION RESEARCH CORPORATION
1720 Randolph Road, S.E.
Albuquerque, New Mexico 87106

TABLE OF CONTENTS

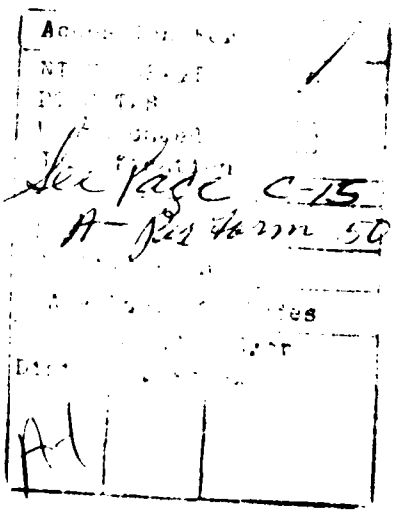

PART A

Overview

Brendan B. Godfrey, Mark M. Campbell,
Barry S. Newberger, and Lawrence A. Wright

Mission Research Corporation
Albuquerque, New Mexico 87106

Until about two years ago it appeared that high current beam propagation in the atmosphere was caught between the proverbial rock and a hard place: Hose stability required a fast risetime pulse, whereas hollowing stability required a slow risetime pulse. Some progress had been made toward eliminating the hollowing instability in fast rising high current beams by means of emittance tailoring[1] and electron energy spread.[2] In addition, there was hope that delta rays might have some salutory effect, such as radial conductivity profile spreading,[3-7] net current enhancement,[4-11] or phase-mix damping.[11] Whether this combination of effects could eliminate hollowing in, for example, a fast rising RADLAC II pulse is, however, unclear.

Fortunately, more recent high current beam propagation studies indicate that the hose instability is not nearly so rapidly growing as had been supposed and that a short risetime pulse is not desirable for hose reduction.[2] This re-assessment of hose behavior permits us to eliminate hollowing simply by increasing the beam risetime.

Part B of this report addresses the question of just how long a current risetime is required to avoid hollowing. Lampe and others at the Naval Research Laboratory (NRL) observed in computer simulations that hollowing in small radius, solid beams is triggered by electron avalanche in air, typically occurring when $E/P > 130$ kV/cm-atm,[12] where E is the beam electric field at the pinchpoint and P is the air density. To facilitate experimental planning we have converted the NRL criterion to an instantaneous current riserate threshold, increasing from about 30 kA/ns-atm in low density air to between 70 and 150 kA/ns-atm in full density air. Of course, nose erosion gradually reduces the risetime of a propagating beam, possibly causing an initially hollowing stable beam to become unstable. We have, therefore, developed a simple analytical argument predicting that a high current beam remains stable over a Nordsieck length provided that its initial risetime in ns exceeds roughly 6/P (atm). A limited set of solid beam simulations presented in Part B support this estimate. More extensive simulations of annular, rotating high current beams give similar results.[13]

The simulations also confirm the ability of electron local energy spread to suppress hollowing.[2] In addition, they suggest that hollowing may arise at lower field strengths in large radius beams than in small, but this possibility does not change our principal conclusions.

The riserate threshold curves presented in Part B were the motivation for IBEX beam experiments performed at low air densities to validate the existing theoretical understanding of hollowing.[14] Computer simulations carried out in support of these experiments are presented in Part C. Agreement between experiment and computation, encompassing open-shutter photographs, autoradiographs, net current measurements, and plasma current decay times, is excellent. Together, the simulations and experiments indicate a hollowing instability threshold of about 120 Torr, consistent with theoretical predictions. The computational study also treats the impact of radius mismatch at injection on the onset of the hollowing instability. Both emittance mismatch and pinching in the diode cause hollowing to occur sooner and with larger amplitude. Finally, low energy beam electrons in the rising portion of the current pulse are found to exacerbate instabilities. Presumably, fewer such electrons will be present in beams produced by multistage accelerators, such as RADLAC and ATA.

Abbreviated presentations of these high current beam hollowing instability results were made at the DARPA-Services Annual Propagation Reviews (Refs. 15-18) and elsewhere.[14,19-23] Other studies performed under Sandia National Laboratories Subcontract 48-1044 but not described here include beam transport and stability in recirculating induction accelerators,[24] an improved air chemistry package for IPROP, numerical methods, and optical diagnostics.

Recent theoretical studies bearing on high current beam propagation supported by other agencies (the Defense Advanced Research Projects Agency and the Air Force Weapons Laboratory) include hollowing instabilities in annular beams,[13] pinching in the IBEX diode,[25] filamentation instabilities in annular beams,[26,27] and the effects of delta rays.[11] Extensive experimental research has been performed as well.[18,28]

REFERENCES

1. K. A. Brueckner, "Beam Propagation and Stability Study," LJI-84-014 (La Jolla Institute, La Jolla, 1984) (S/NSI).

2. R. R. Johnston, D. A. Keeley, C. L. Yee, B. B. Godfrey, L. Wright, T. Hughes, and N. Carron, "Charged Particle Beam Propagation Studies," SAI-C-57-PA (Science Applications Inc., Palo Alto, 1983) (S/NSI).

3. B. B. Godfrey, "High Current Beam Propagation Study," AMRC-R-367 (Mission Research Corporation, Albuquerque, 1982).

4. N. Carron and W. Wortman, "Nonlocal Ionization in Charged Particle Beams," MRC-R-649 (Mission Research Corporation, Santa Barbara, 1981) (S/NSI).

5. K. A. Brueckner, "Beam Propagation and Stability," LJI-81-145 (La Jolla Institute, La Jolla, 1981) (S/NSI).

6. R. R. Johnston, R. L. Feinstein, and D. A. Keeley, "Theoretical Study in Charged Particle Beam Propagation," SAI-C-46-PA (Science Applications Inc., Palo Alto, 1981) (S/NSI).

7. R. R. Johnston, R. L. Feinstein, D. A. Keeley, and H. R. Kirch, "Theoretical Study in Charged Particle Beam Propagation," SAI-C-51-PA (Science Applications Inc., Palo Alto, 1981) (S/NSI).

8. S. S. Yu and R. E. Melendez, "Delta-Ray-Coupled-Hose Instability I: Mathematical Framework," UCRL-91412 (Lawrence Livermore National Laboratory, Livermore, 1983).

9. S. S. Yu, R. E. Melendez, and F. W. Chambers, "Delta-Ray-Coupled-Hose Instability II: Dispersion Relation," UCRL-91413 (Lawrence Livermore National Laboratory, Livermore, 1983).

10. S. S. Yu and R. E. Melendez, "Delta-Ray-Coupled-Hose Instability III: Code Results," UCRL-91414 (Lawrence Livermore National Laboratory, Livermore, 1984).

11. L. A. Wright, unpublished (1985).

12. M. Lampe and G. Joyce, "Axisymmetric Instabilities of a Propagating Electron Beam," NRL-5015 (Naval Research Laboratory, Washington, 1983) (S/NSI).

13. N. F. Roderick, "Axisymmetric Hollowing Instability in Rotating Annular Beams," AMRC-R-622 (Mission Research Corporation, Albuquerque, 1985).

14. C. A. Ekdahl, J. R. Freeman, G. T. Leifeste, R. B. Miller, W. B. Styger, and B. B. Godfrey, submitted to Phys. Rev. Lett. (1985).

15. DARPA/Services Annual Propagation Review, Session Summaries, CONF-8306158 (Lawrence Livermore National Laboratory, Livermore, 1984) (S/NSI).

16. B. B. Godfrey, R. J. Adler, M. M. Campbell, N. J. Carron, T. P. Hughes, G. F. Kiuttu, N. F. Roderick, and L. A. Wright, "Presentation to DARPA/Services Propagation Review," AMRC-N-232 (Mission Research Corporation, Albuquerque, 1983).

17. DARPA/Services Annual Propagation Review, Proceedings, CONF-8406133 (Lawrence Livermore National Laboratory, Livermore, 1984) (S/NSI).

18. B. B. Godfrey, R. J. Adler, T. P. Hughes, G. F. Kiuttu, D. Mitrovich, R. J. Richter-Sand, N. F. Roderick, D. J. Sullivan, and L. A. Wright, "Presentation to DARPA/Services Propagation Review," AMRC-R-592 (Mission Research Corporation, Albuquerque, 1984).

19. B. B. Godfrey, Bull. Am. Phys. Soc. 29, 1291 (1984).

20. C. A. Ekdahl, W. B. Styger, G. T. Leifeste, J. R. Freeman, R. B. Miller, and B. B. Godfrey, Bull. Am. Phys. Soc. 29, 1377 (1984).

21. R. Gullickson and C. M. Huddleston (Eds.), DARPA/NAVY Charged Particle Beam Technology Progress Report 33 (Naval Surface Weapons Center, White Oak, 1983), p. 15-17 (S/NSI).

22. R. Gullickson and C. M. Huddleston (Eds.), DARPA/NAVY Charged Particle Beam Technology Progress Report 35 (Naval Surface Weapons Center, White Oak, 1984), p. 17 - 19 (S/NSI).

23. R. Gullickson and C. M. Huddleston (Eds.), DARPA/NAVY Charged Particle Beam Technology Progress Report 36 (Naval Surface Weapons Center, White Oak, 1984), p. 22 - 24 (S/NSI).

24. L. A. Wright, in preparation (1985).

25. D. E. Pershing, C. A. Sedlak, R. H. Jackson, M. M. Campbell, and B. B. Godfrey, "Simulation of the IBEX Diode with SCRIBE," MRC/WDC-R-082 (Mission Research Corporation, Washington, 1984).

26. T. P. Hughes and H. S. Uhm, "Resistive Instabilities in a Thick, Hollow Electron Beam," AMRC-R-543 (Mission Research Corporation, Albuquerque, 1984).

27. H. S. Uhm and T. P. Hughes, "Filamentation Instability of a Self-Pinched Hollow Electron Beam," MP-84-230 (Naval Surface Weapons Center, White Oak, 1984).

28. R. J. Adler, G. F. Kiuttu, and R. J. Richter-Sand, "Stabilization of the Resistive Hose Instability in Intense Electron Beams," AMRC-R-598 (Mission Research Corporation, Albuquerque, 1984) (S/NSI).

PART B

Hollowing Instability Threshold Determination

Brendan B. Godfrey

Mission Research Corporation
Albuquerque, New Mexico 87106

I. INTRODUCTION AND SUMMARY

High current relativistic electron beams propagating in air are subject to a variety of macroscopic resistive instabilities, including hollowing, hose, and filamentation. Although the hose instability typically dominates experiments,[1-8] computer simulations indicate that hollowing is potentially very disruptive to fast current risetime beams, especially at low air density.[9-14] There have, moreover, been at least three experiments which exhibited the hollowing instability clearly.[15-18] Results from the last of these, performed using the 4 MeV, 70 kA IBEX beam generator, are analysed in Part C of this report.

In a typical hollowing instability simulation, a region of reduced beam current density develops on the beam axis immediately behind the pinch point. (The pinch point, located near the front of the beam, is marked by an inductive spike in the axial electric field as the beam pinches rapidly due to space-charge neutralization by ionization of the background air.) The reduced density region convects back in the beam pulse and gradually damps, only to be replaced by a still larger density reduction just behind the pinch point. This process typically continues until the front of the beam blows apart, although in a few instances the beam has been observed in simulations to evolve to a stable hollow configuration.[14],[16] It is also possible for beam parameters to change sufficiently before the instability has reached a nonlinear amplitude that the beam is no longer unstable, and the instability then decays away.

This hollowing of the beam current profile drives, and is in turn driven by, eddy currents in the resistive background plasma. Net (i. e., beam plus plasma) currents reverse locally for well developed hollowing. It is the phase lag between beam and plasma oscillations that causes the instability. The hollowing mode frequency in the laboratory frame is several times the inverse of the monopole current decay time,

$$\tau_M = 4\pi \sigma a^2/c^2 \qquad (1)$$

while the typical growth rate is an order of magnitude smaller.[12] In Eq. (1), σ is the plasma conductivity, and a is the beam radius. The beam frame frequency is approximately the betatron frequency,

$$\Omega_\beta = \frac{c}{a}\left(\frac{\nu_n}{\gamma}\right)^{1/2} \qquad (2)$$

where ν_n is the net current normalized to 17 kA, and γ is the electron energy. No fully satisfactory analytical treatment of the relativistic electron beam hollowing instability exists, although some useful idealized analyses have been performed.[19]

The hollowing instability is triggered by strong peaking on axis of the plasma equilibrium conductivity and return current profiles. A high plasma conductivity localized to the region of the beam axis can be caused by avalanche ionization of the air in the beam inductive electric field at the pinch point. Extensive detailed simulations by Joyce and coworkers indicate that hollowing occurs when the ratio of the electric field to the air density exceeds 130 kV/cm-atm. In addition, the plasma return current must exceed one-half the beam current in magnitude.[11] Usually, but not always, the first condition implies the second.

For experimental purposes it is necessary to relate the instability threshold criteria to quantities which can be controlled in the laboratory. To lowest order the peak inductive electric field is proportional to the rate of current rise in the beam front. In Sec. III we express numerically the 130 kV/cm-atm requirement in terms of the instantaneous current rise rate and the air pressure for a wide range of parameters. The results are found to depend only weakly on beam radius and not at all on the beam current. For the IBEX beam with a 15 ns risetime, the hollowing instability is expected to develop at pressures of about 80 Torr and below.

An initially stable beam may become hollowing unstable during propagation due to nose erosion and consequent risetime reduction. A simple analytical estimate of this effect is derived in Sec. IV. It predicts that a high current beam in uniform air remains stable over at least a Nordsieck length provided its initial risetime is sufficiently large:

$$\tau_r \text{ (ns)} \sim 6/P \text{ (atm)} \qquad (3)$$

The Nordsieck length is the distance over which the radius of a self-pinched electron beam expands by an e-fold due to atomic scattering.[20-22]

Six simulations discussed in Sec. V confirm the qualitative features of our erosion induced instability model but indicate that it is too pessimistic by a factor of two for propagation in full density air. In addition, the simulations display two unexpected features. For beam radii in the range of 1.0 to 1.5 cm (after some Nordsieck expansion), hollowing instabilities occur at pinch point field strengths as low as 75 kV/cm-atm. Beam simulations just above the instability threshold exhibited a weak hollowing after several meters of propagation which subsequently damps, presumably due to an increase in the beam local energy spread. These results deserve further investigation.

CPROP, the numerical simulation code used in this study, is described in Sec. II, which follows.

II. NUMERICAL METHODS

CPROP is a two-dimensional beam simulation code designed for investigating the axisymmetric dynamics of high current relativistic electron beam propagation in air. It is based on the general purpose, relativistic, electromagnetic, particle-in-cell (PIC) code CCUBE, and thus possesses most of the diagnostic and other capabilities of that program.[23] Three major enhancements to CCUBE were required to treat beam transport in air: an electromagnetic field solver accommodating arbitrary scaler conductivity and a moving coordinate mesh, a conductivity generation package, and a Moliere electron scattering routine. Each of these is discussed below, with the field solver receiving most attention. CPROP also contains a high energy delta-ray generation and transport package, but it was not employed in the present investigations. Delta rays do not seem to have an important effect on the hollowing instability.[24]

Most PIC propagation codes utilize the so-called frozen field approximation.[11,14,25] The electrostatic potential and the axial component only of the vector potential are evaluated in a (Galalean transformed) frame moving with the beam at the speed of light; the forward-going characteristic light line is dropped.[26] Consistent with this assumption, particle dynamics are treated in the high energy, paraxial limit. This approach works well for highly relativistic beams and saves a small amount of computer time and a significant amount of computer memory. It is, however, not so well suited for moderate energy laboratory beams, such as IBEX. Also, the accuracy of the frozen-field approximation near metallic axial boundaries (e.g., drift tube endplates) is unclear. As a consequence, we have chosen to accept the higher costs of a more complete treatment of the field and particle equations in order to simulate laboratory experiments better.

A field algorithm suitable for beam propagation in air must be numerically accurate and stable for arbitrarily large or small conductivities, have a non-restrictive Courant limit on the time step, and accommodate computations in both the laboratory and beam frames. An algorithm, based on earlier work by

Longmire[27] and by Feinstein[28] has been developed to satisfy these requirements. Maxwell's equations for E_z, E_r, and B_θ (the only fields needed for axisymmetric transport of nonrotating particle beams) are recast in coupled forward- and backward-going wave equations.[29]

$$\left[\frac{\partial}{\partial t} + (1 - v)\frac{\partial}{\partial z}\right](E_r + B_\theta) + \sigma E_r = - J_r + \frac{\partial}{\partial r} E_r \tag{4}$$

$$\left[\frac{\partial}{\partial t} - (1 + v)\frac{\partial}{\partial z}\right](E_r - B_\theta) + \sigma E_r = - J_r + \frac{\partial}{\partial r} E_r \tag{5}$$

$$\left[\frac{\partial}{\partial t} - v\frac{\partial}{\partial z}\right] E_z + \sigma E_z = - J_z + \frac{1}{r}\frac{\partial}{\partial r} r B_\theta \tag{6}$$

with v the axial mesh velocity, normalized to the speed of light and assumed positive. The beam current J and the conductivity σ are normalized to contain a factor of 4π. These equations are then partially integrated along the axial characteristics and finite differenced both axially and radially. A three-dimensional version of the algorithm also exists.[24]

We further refine the algorithm by demanding that its dispersion relation for electromagnetic waves in a homogeneous resistive medium share certain properties with the exact analytical dispersion relation. Specifically, we require that the dispersion relation factor into electrostatic and electromagnetic terms and that the wave damping rates be correct, each in the limit of vanishing radial but finite axial cell dimensions. The rates are equal to σ for the electrostatic mode, and σ and k^2/σ for the two electromagnetic modes; k is the wavenumber.

The resulting finite difference equations are

$$\begin{aligned} & E_r^{n+1,i}\left[\frac{1}{2}\left(1 + \frac{\Delta t}{\tau_2}\right) + \frac{\Delta t}{\tau_1}\left(e^{\sigma\tau_1} - 1\right)\right] + B_\theta^{n+1,i}\ \frac{1}{2}\left(1 - \frac{\Delta t}{\tau_2}\right) \\ & = \frac{\Delta t}{\tau_2}\ \frac{1}{2}\left(1 - W_2\right)\left(E_r^{\mu} - B_\theta^{\mu}\right) + \frac{\Delta t}{\tau_2}\ \frac{1}{2} W_2\left(E_r^{n,i+1} - B_\theta^{n,i+1}\right) \\ & + \frac{1}{2}\left(1 - W_1\right)\left(E_r^{n,i} + B_\theta^{n,i}\right) + \frac{1}{2} W_1\left(E_r^{n,i-1} + B_\theta^{n,\ i-1}\right) \\ & - \frac{\Delta t}{\tau_1}\ \frac{1}{\sigma}\left(e^{\sigma\tau_1} - 1\right) J_r^{n+1,i} \end{aligned} \tag{7}$$

$$E_r^{n+1,i}\ \frac{1}{2}\left(1 - \frac{\Delta t}{\tau_2}\right) + B_\theta^{n+1,i}\ \frac{1}{2}\left(1 + \frac{\Delta t}{\tau_2}\right) - \frac{\partial}{\partial r}\ E_z^{n+1,i}\ \Delta t$$

$$= -\frac{\Delta t}{\tau_2}\ \frac{1}{2}\left(1 - W_2\right)\left(E_r^{\mu} - B_\theta^{\mu}\right) - \frac{\Delta t}{\tau_2}\ \frac{1}{2}\ W_2\left(E_r^{n,i+1} - B_\theta^{n,i+1}\right)$$

$$+ \frac{1}{2}\left(1 - W_1\right)\left(E_r^{n,i} + B_\theta^{n,i}\right) + \frac{1}{2}\ W_1\left(E_r^{n,i-1} + B_\theta^{n,i-1}\right) \qquad (8)$$

$$E_z^{n+1,i}\left[\frac{1}{2}\left(1 + \frac{\Delta t}{\tau_2}\right) + \frac{\Delta t}{\tau_1}\left(e^{\sigma\tau_1} - 1\right)\right] - \frac{\Delta t}{\tau_1}\ \frac{1}{\sigma}\left(e^{\sigma\tau_1} - 1\right)\frac{1}{r}\ \frac{\partial}{\partial r}\ rB_\theta^{n+1,i}$$

$$= \frac{\Delta t}{\tau_2}\ \frac{1}{2}\left(1 - W_2\right) E_z^{\mu} + \frac{\Delta t}{\tau_2}\ \frac{1}{2}\ W_2\ E_z^{n,i+1}$$

$$+ \frac{1}{2}\left(1 - W_1\right) E_z^{n,i} + \frac{1}{2}\ W_1\ E_z^{n,i+1}$$

$$- \frac{\Delta t}{\tau_1}\ \frac{1}{\sigma}\left(e^{\sigma\tau_1} - 1\right) J_z^{n+1,i} \qquad (9)$$

where

$$\tau_1 = \min\left(\frac{\Delta z}{v}\ ,\ \Delta t\right)\ ;\quad \tau_2 = \min\left(\frac{\Delta z}{1+v}\ ,\ \Delta t\right) \qquad (10)$$

$$W_1 = \frac{(1-v)\Delta t}{\Delta z}\ ;\quad W_2 = \min\left(\frac{\Delta z}{(1+v)\Delta t}\ ,\ \frac{(1+v)\Delta t}{\Delta z}\right) \qquad (11)$$

and the index pair μ is given by (n+1,i+1) or (n,i) depending on whether τ_2 assumes its first or second value in Eq. (10). In the equations Δt is the time step and Δz is the axial cell size. The indices n and i indicate time step and axial cell numbers, respectively, with i increasing from the tail of the beam to the head. See Fig. 1.

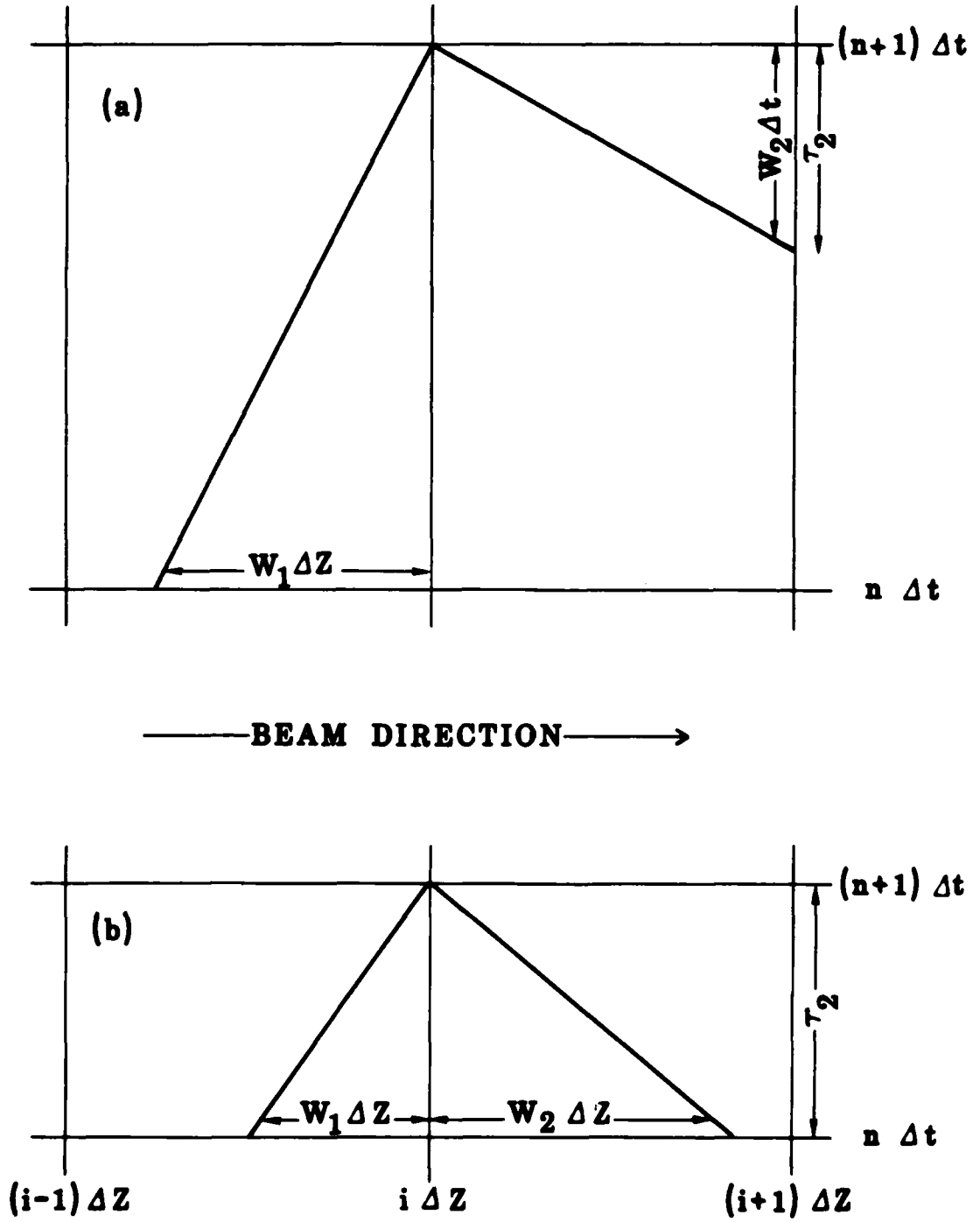

Figure 1. Typical z-t coordinate meshes for (a) $\Delta z < (1+v)\Delta t$, and (b) $\Delta z > (1+v)\Delta t$. Forward- and backward-going light lines, interpolation quantities W_1 and W_2, and forward light line integration time τ_2 also are shown. Omitted are the conductivity characteristic and integration time τ_1.

Centered radial differences are represented by differentials in Eqs. (9)-(11) for notational simplicity. E_r and B_θ are located radially at cell edges, and E_z is located at cell centers. As boundary conditions the two former fields are required to vanish on axis, while the latter field is set to zero at the outer radial edge of the mesh, far from the beam. Fields on the axial boundary ahead of the beam are set to zero. Fields on the rear axial boundary depend on the problem simulated.

Various nonuniform zonings are accommodated by the difference equations. We have found that a radial cell size uniform in the coordinate ξ,

$$\xi = a \ln(1 + r/a) \tag{12}$$

with a the nominal beam Bennett radius, works well. It results in cells uniform in size within the beam and expanding linearly with larger radii. Both uniform and linear zoning, starting from the beam front, have been employed in the axial direction.

Equations (7)-(9) are solved numerically at each time step by sweeping axially from the head of the beam back (i.e., decreasing i). At each axial slice the right sides of the equations are evaluated from quantities already known from either the preceding time step or the axial disk next further forward in the beam, as indicated in Fig. 1. E_r is then eliminated from the left sides of the equations, and E_z and B_θ are evaluated by tridiagonal reduction. Finally, E_r is computed by back substitution. The procedure is straight-forward and reasonably fast.

The Courant condition associated with Eqs. (9)-(11) is

$$\Delta t < \Delta z/(1-v) \tag{13}$$

For v near unity, Δt is instead constrained by particle dynamics, as in the frozen field approximation.

Note that the CPROP field solver is prone to charge continuity errors, because the radial field variation is treated implicitly while the axial variation is not. These errors, which accumulate slowly, are of no concern in beam propagation simulations. Air conductivity quickly swamps them. Even without conductivity, continuity errors would fall off the end of the moving coordinate mesh before they could grow to worrisome magnitudes.

Conductivity is computed using the BMCOND air chemistry package.[30] It follows the time histories of the plasma electron density and temperature and of the densities of several ionic species. The electron momentum transfer cross section and other key coefficients are temperature dependent. The model equations respond to the beam through impact ionization and ohmic return current heating. BMCOND has been calibrated against more extensive air chemistry codes; it is quite accurate for parameter regimes of interest.

Properly treating beam electron scattering on air molecules is central to calculating correctly beam radial expansion[21-22] and nose erosion rates,[31-32] both important to our hollowing instability study. The usual Rossi-Greisen[33] scattering formalism is inadequate for lower energy beams. Instead, we use Moliere scattering,[34] which consists basically of Williams scattering[35] at small angles and Coulomb scattering at large.[36] Moliere scattering leads to a smaller radial expansion rate combined with a very slow loss of beam particles. The impact of various scattering models on computed Nordsieck lengths, including comparisons with experiment, is described in greater detail elsewhere.[22] Scattering is implemented in CPROP by applying a deflection to the beam electrons every so many time steps. The deflection angle is chosen randomly from a large set of previously computed small angles forming a truncated Moliere distribution or from an analytical expression for occasional large angles. Other aspects of the CPROP particle dynamics are as in CCUBE.

III. INSTANTANEOUS CURRENT RISERATE THRESHOLDS

Numerous short CPROP runs were carried out to determine current riserates corresponding to the Naval Research Laboratory 130 kV/cm-atm hollowing instability threshold. Simulations were performed at air densities of 0.03, 0.1, 0.3, and 1.0 atm for beams currents of 20, 40, and 100 kA and matched radii of 0.5 and 2.0 cm. We did not extend our calculations below 20 Torr, because the air chemistry model is inaccurate there. Beams were initialized with current axial profiles

$$I = I_0 \tanh (\tau/\tau_r) \tag{14}$$

and various risetimes τ_r. A Bennett radial profile was assumed,

$$J_z = \frac{I}{\pi a^2}\left(1 + \frac{r^2}{a^2}\right)^{-2} \tag{15}$$

with the Bennett radius flared by a factor of two in the beam nose to take account of reduced pinching there.

$$a = a_0 \left[2 - \tanh (\tau/\tau_r)\right] \tag{16}$$

Simulations were performed in the beam frame with particle positions held fixed in that frame to eliminate erosion effects and to reduce computer costs.

Results are summarized in Fig. 2, which shows threshold current riserates verses air density. Threshold values for the three currents are indistinguishable. We do not expect this invariance to persist much below 20 kA, but hollowing is much less a problem at lower currents. Variation of the threshold with beam radius also is weak. Throughout the parameter range considered, the net current behind the pinch point exceeded half the beam current whenever the riserate threshold was met.

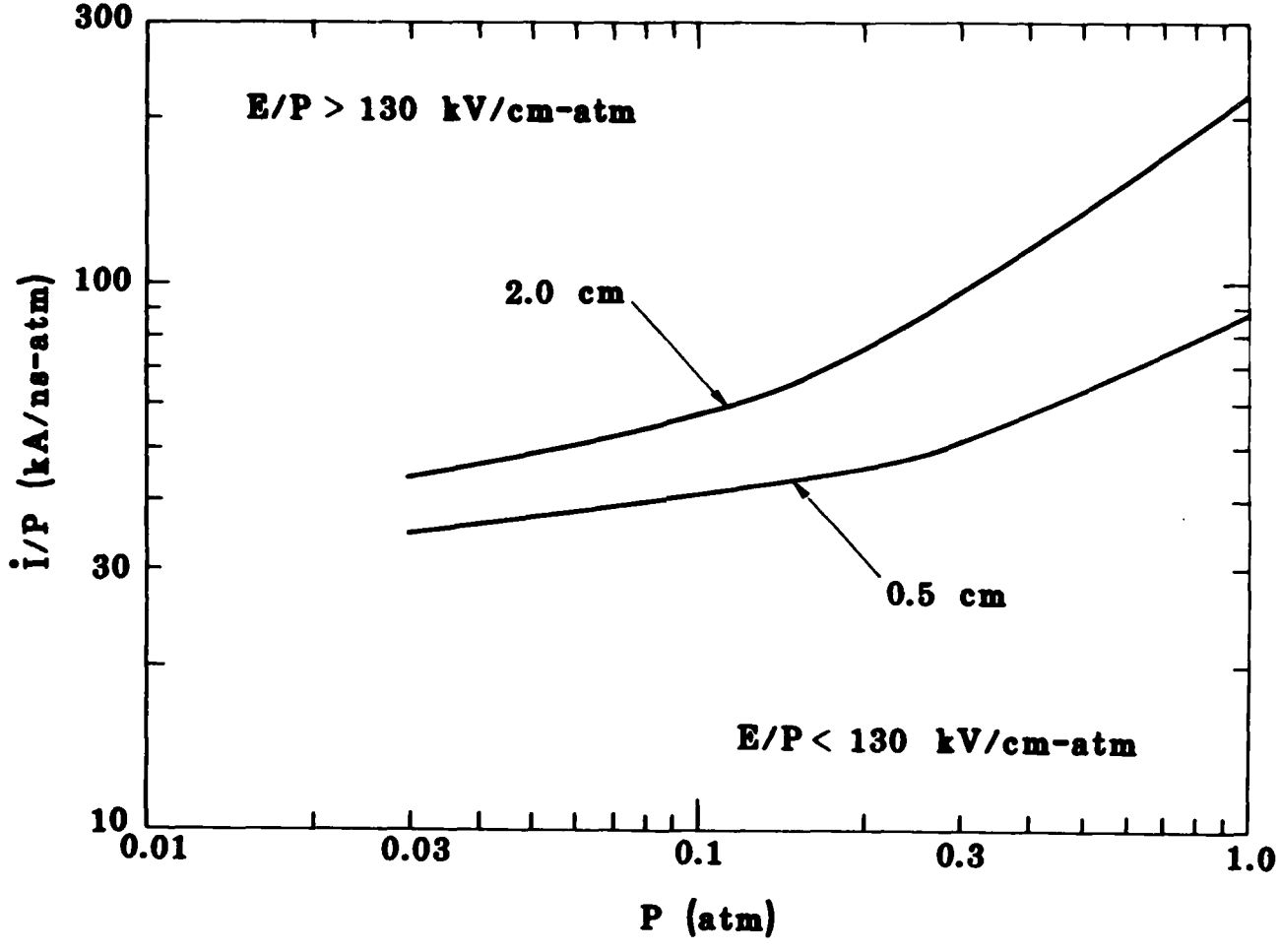

Figure 2. Beam current riserates corresponding to E/P = 130 kv/cm-atm for 0.5 and 2.0 cm radius beams.

IV. EROSION EFFECT ESTIMATE

A beam initially stable according to Fig. 2 may become unstable after propagating some distance due to pulse sharpening from erosion. The pulse sharpening process is shown schematically in Fig. 3. Leaving the accelerator, the beam has a linearly rising current profile of length τ_r. The pinch point is located a distance τ_i behind the beam front, and the current is I_i there. The leading portion of the pulse erodes away during propagation, causing the effective risetime to decrease. In addition, the pinch point moves back into the pulse to a distance τ_f from the initial beam front, where the current is larger, I_f. Both effects push the beam toward instability.

The erosion rate for high current beams scales roughly as[12,31-32]

$$\frac{d\tau}{dt} \approx 6 \frac{\nu_n}{\gamma} \frac{\tau}{\tau_r} \tag{17}$$

during the linearly rising portion of the current pulse. We assume that the net current is proportional to the beam current over enough of the rising portion of the beam pulse to make our calculation reasonable.

The Nordsieck length is an attractive distance for which to demand beam stability, since at much greater distances the beam current density drops significantly due to radial expansion. For sufficiently high beam power, the Nordsieck length is given by[21-22]

$$L_N \text{ (m)} = 0.4 \nu_n \gamma/P \text{ (atm)} \tag{18}$$

Integrating Eq. (17) over a Nordsieck length and replacing τ_f/τ_i by I_f/I_i then yields

$$\ln\left(\frac{I_f}{I_i}\right) = 6 \frac{\nu_n}{\gamma} \frac{L_N}{\tau_r} \tag{19}$$

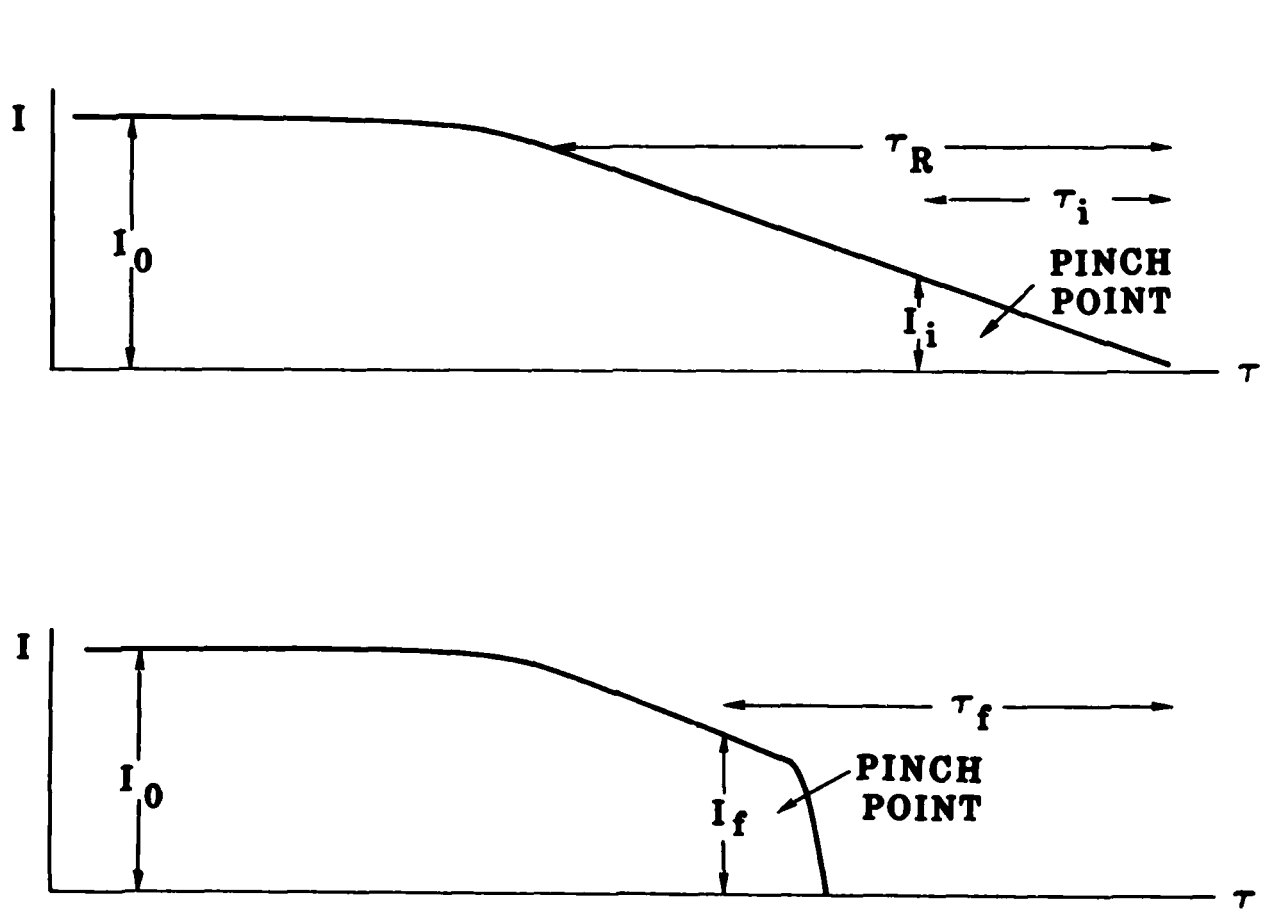

Figure 3. Hypothetical beam current profile (a) before, and (b) after nose erosion. I_i and I_f are the initial and final currents at the beam pinch point, and τ_i and τ_f are the corresponding positions of the pinch point relative to the initial front of the beam.

Unfortunately, Eq. (19) says nothing about the effective pulse risetime after erosion, which would be needed to apply the curves in Fig. 2 to this analysis. Instead, we rely on the fact that hollowing tends to occur in simulations of fast rising current beams when the beam current at the pinch point exceeds about 17 kA in full density air. The current at which the pinch point forms in slow rising current beams when injected into full density air is seen in simulations to be a few to several kA. Hence, $\ell n(I_f/I_i) \approx 1\text{-}2$. This factor may decrease a bit at reduced densities, but the dependence should be weak, because a logarithm is involved. Estimating the normalized net current is easier. It saturates at $\nu_n \approx 1$ for high beam currents, independent of most anything else. Inserting these values into Eq. (19) and solving for τ_r leads to the beam risetime threshold in Eq. (3). Simulations refining this estimate are presented in the next section.

V. NUMERICAL SIMULATIONS

Six CPROP simulations of an initially 35 MeV, 70 kA, 0.8 cm radius electron beam in 1.0 or 0.1 atm air were performed to study hollowing in slowly rising current pulses. The beam current and matched radius were chosen to approximate that of the IBEX beam. The electron energy was, however, increased by an order of magnitude in order to make the hollowing instability onset more gradual and, therefore, easier to observe. The pulse shape was initialized according to Eqs. (14)-(16). The transverse velocity distribution was locally Maxwellian with an axially varying temperature chosen to produce a constant beam emittance.

The six runs are summarized in Table 1. Listed are the current risetime for each case, the air density, and, except for Cases 3 and 4, the propagation distance at which hollowing was first visible. Cases 3 and 4 showed no disruptive hollowing and were terminated after 20 m, approximately a Nordsieck length. Thus, the full density air simulations give a riserate threshold more optimistic than Eq. (3) by about a factor of two. Initial risetimes in the one-tenth air density simulations, Cases 5 and 6, bracket the instantaneous threshold curves in Fig. 2 and, therefore, do not provide a good test of Eq. (3). They do, on the other hand, lend additional credence to the curves. Simulations at one-tenth atmosphere demonstrating stability over a 200 m Nordsieck length would be prohibitively expensive. Individual simulations are discussed in more detail below.

Case 1, with $\dot{I}/P$ = 70 kA/ns-atm, was initially within 50% of the hollowing instability instantaneous threshold value from Fig. 2. The pinch point inductive electric field rose from 80 to 130 kV/cm within the first 1.2 m of propagation. Hollowing was well developed at 2 m and had destroyed the beam head by 4.5 m.

Hollowing was not evident in Case 2 until about 3.3 m of propagation. Interestingly, the peak axial electric field had risen only to 95 kV/cm at that point, somewhat below the expected 130 kV/cm value. The pinched beam radius

TABLE 1. PROPAGATION LENGTH FOR ONSET OF HOLLOWING INSTABILITY

(Cases 3 and 4 were terminated after one Nordsieck length with no disruptive hollowing.)

CASE	CURRENT RISETIME (ns)	AIR DENSITY (atm)	PROPAGATION LENGTH (m)
1	1	1.0	1
2	2	1.0	3
3	3	1.0	20
4	4	1.0	20
5	10	0.1	1
6	20	0.1	4

had expanded to about 0.95 cm. It may be that the published E/P threshold, which was obtained primarily from simulations of lower current, smaller radius beams,[11-14] is too high for the present beam parameters. If so, the upper curve in Fig. 2 should lie much closer to the lower curve. Discrepancies of this magnitude are not, in general, critical for experimental comparisons.

Case 3 is particularly striking. A weak but distinct hollowing instability developed after 5 m of propagation and persisted until about 15 m, when it decayed away. The peak electric field ranged between 75 and 90 kV/cm during this period. The instability did not disrupt the beam, although it may have enhanced nose erosion and expansion slightly. We attribute this very slow growth and subsequent damping of the hollowing instability to a local spread in betatron frequencies resulting from a spread in electron energies. Beam electrons loose energy primarily to the axial inductive electric field maintained by the gradual resistive decay of the plasma return current. Behind the pinch point this field is a few tens of kV/cm on axis and drops off rapidly with radius. (In contrast, energy loss by atomic collisions amounts to only 2-3 keV/cm in full density air.) Depending on their orbits, beam electrons sample different average field strengths and so loose differing amounts of energy. In this simulation electrons originally 3 m behind the front of the beam lost an average of 12 MeV during nearly 20 m of propagation. The corresponding energy

spread half-width was roughly 6 MeV. An earlier study[12] suggests that a 15% local energy spread is sufficient to suppress hollowing in 20 kA beams. A 15% spread had developed in Case 3 by 12 m. It should also be noted that the hollowing instability frequency (in the beam frame) changed by a factor of two during the run due to evolving conditions in the beam nose. This, too, may have had a stabilizing effect.

Qualitatively, Case 4 was quite similar to Case 3. The beam was very weakly hollowing unstable at a distance of 15 to 17 m. The peak electric field was 85 kV/cm at that point. Because this simulation was least affected by instabilities, it provides the clearest picture of the evolution of the beam equilibrium. Some 3 ns of beam pulse was eroded during 20 m of propagation, as indicated in Fig. 4. The beam radius 2 m behind the initial beam front increased by an e-fold. Beam expansion well behind the pinch point was caused primarily by atomic scattering, with lesser contributions from electron energy loss and the weak instability.

With $\dot{I}/P$ = 70 kA/ns-atm, Case 5 was well above the Fig. 2 instability threshold for 0.1 atm. The beam became unstable almost immediately and was severely disrupted after 8 m. The peak electric field ranged between 15 and 28 kV/cm.

Case 6, on the other hand, fell about 35% below the threshold. Hollowing was first visible, about 3 m behind the pinch point, after 4 m of propagation. The instability grew slowly, causing serious disruption at 12 m. The pinch point electric field was close to 21 kV/cm throughout this period. Note that hollowing stabilization by local energy spread can occur in an initially monoenergetic beam only after traveling proportionately much greater distances at this low air density.

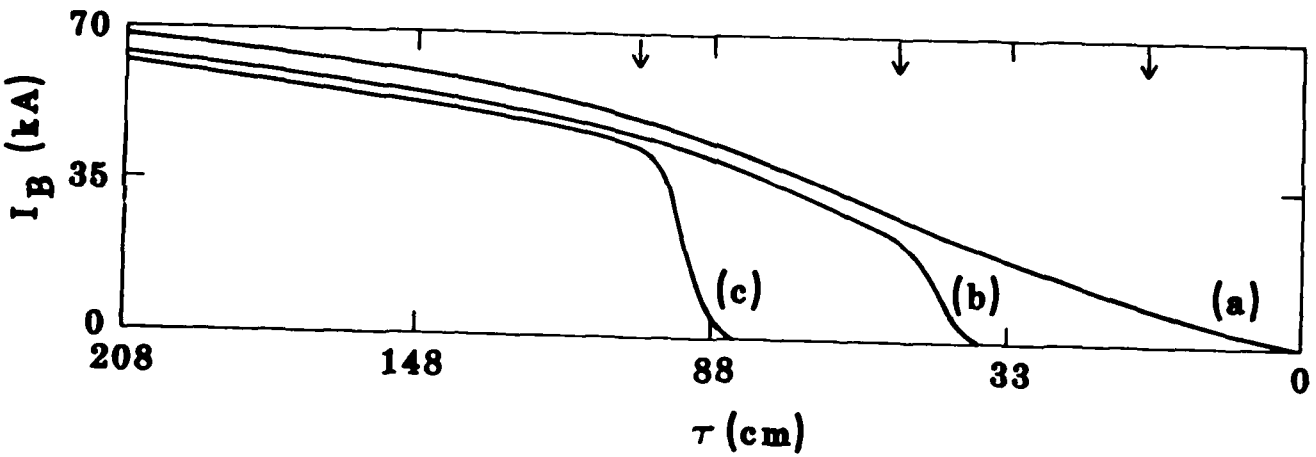

Figure 4. Beam current axial profiles for Case 4 after (a) 0 m, (b) 10 m, and (c) 19 m of propagation. The corresponding pinch point positions are indicated as well. Note the nonlinear distance scale in the plot.

ACKNOWLEDGEMENTS

The author is endebted to R. B. Miller for suggesting these calculations and to him, R. L. Feinstein, and C. A. Ekdahl for useful suggestions.

This research was supported by the Sandia National Laboratories, Albuquerque and by the Defense Advanced Research Projects Agency (contract monitored by the Naval Surface Weapons Center, White Oak).

REFERENCES

1. R. J. Briggs, J. C. Clark, T. J. Fessenden, R. E. Hester, E. J. Lauer, in High Power Electron and Ion Beams (J. A. Nation and R. N. Sudan, Eds.), Vol. I, p. 319 (Ithaca, 1977).

2. E. J. Lauer, R. J. Briggs, T. J. Fessenden, R. E. Hester, and E. P. Lee, Phys. Fluids 21, 1327 (1978).

3. R. B. Fiorito, R. F. Fernsler, J. R. Greig, M. Herndon, I. M. Vitkovitsky, A. W. Ali, and V. E. Scherrer, "An Initial Study of the Injection of an Intense Relativistic Electron Beam into the Atmosphere," NRL-4405 (Naval Research Laboratory, Washington, 1981).

4. R. B. Fiorito, E. W. Fordham, J. R. Greig, R. E. Pechacek, J. D. Sethian, R. F. Fernsler, and J. C. Halle, "Dynamics of an Intense Relativistic Electron Beam Injected into Full Density Air," NRL-4557 (Naval Research Laboratory, Washington, 1981).

5. M. A. Greenspan, "Short-Pulse Electron-Beam Propagation Experiments in a Controlled-Environment Chamber," MDC Q0762 (McDonnell-Douglas Research Laboratories, St. Louis, 1982).

6. M. A. Greenspan and E. A. Rose, "Investigation of Short-Pulse Electron-Beam Propagation," MDC Q1208 (McDonnell-Douglas Research Laboratories, St. Louis, 1983).

7. R. J. Adler, G. F. Kiuttu, and B. Sabol, in Beams '83: High Power Particle Beams (R. J. Briggs and A. J. Toepfer, Eds.), p. 366 (San Francisco, 1983).

8. R. J. Adler, G. F. Kiuttu, and R. J. Richter-Sand, "Stabilization of the Resistive Hose Instability in Intense Electron Beams," AMRC-R-598 (Mission Research Corporation, Albuquerque, 1984).

9. F. W. Chambers, "Sausage Mode Stability Boundaries: Enumeration and Verification," UCID-18879 (Lawrence Livermore National Laboratory, Livermore, 1980).

10. B. B. Godfrey, "High Current Beam Propagation Study," AMRC-R-367 (Mission Research Corporation, Albuquerque, 1982).

11. G. Joyce and M. Lampe, Phys. Fluids 26, 3377 (1983).

12. R. R. Johnston, D. A. Keeley, C. L. Yee, B. B. Godfrey, L. Wright, T. Hughes, and N. Carron, "Charged Particle Beam Propagation Studies," SAI-C-57-PA (Science Applications Inc., Palo Alto, 1983) (S/NSI).

13. G. Joyce, M. Lampe, R. R. Hubbard, and R. Fernsler, in Beams '83: High Power Particle Beams (R. J. Briggs and A. J. Toepfer, Eds.), p. 382 (San Francisco, 1983).

14. K. A. Brueckner, private communication (1983).

15. C. A. Ekdahl, "Beam Propagation Experimental Study," AMRC-R-352 (Mission Research Corporation, Albuquerque, 1982).

16. R. J. Adler, G. F. Kiuttu, B. A. Sabol, W. Bostick, C. A. Ekdahl, L. A. Wright, B. B. Godfrey, T. P. Hughes, N. F. Roderick, and D. J. Sullivan, "Beam Propagation Experimental Study," AMRC-R-466 (Mission Research Corporation, Albuquerque, 1983).

17. C. A. Ekdahl, J. R. Freeman, G. T. Leifeste, R. B. Miller, W. B. Styger, and B. B. Godfrey, submitted to Phys. Rev. Lett. (1985).

18. B. B. Godfrey, in Proc. DARPA-Services Annual Propagation Physics Review, CONF-8406133 (Monterey, 1984) (S/NSI).

19. H. S. Uhm and M. Lampe, Phys. Fluids 25, 1444 (1982).

20. A. Nordsieck, unpublished (1959).

21. E. P. Lee, Phys. Fluids 19, 60 (1976).

22. T. P. Hughes and B. B. Godfrey, Phys. Fluids 27, 1531 (1984).

23. L. E. Thode, B. B. Godfrey, and W. R. Shanahan, Phys. Fluids 22, 749 (1979).

24. B. B. Godfrey and L. A. Wright, unpublished (1985).

25. F. W. Chambers, "Mathematical Models for the Ringbearer Simulation Code," UCID-18302 (Lawrence Livermore National Laboratory, Livermore, 1979).

26. E. P. Lee, "The New Field Equations," UCID-17286 (Lawrence Livermore National Laboratory, Livermore, 1976).

27. C. L. Longmire, "Electromagnetic Fields near the Head of a Relativistic Electron Beam," MRC-R-341 (Mission Research Corporation, Santa Barbara, 1977).

28. R. L. Feinstein, private communication (1981).

29. B. B. Godfrey, in Proc. Tenth Conf. Numerical Simulation of Plasmas, paper 1C6 (San Diego, 1983).

30. R. L. Feinstein, "BMCOND Model," SAI-U-080-8203 (Science Applications Inc., Palo Alto, 1982).

31. E. P. Lee, "Model of Beam Head Erosion," UCID-18768 (Lawrence Livermore National Laboratory, Livermore, 1980).

32. W. M. Sharp and M. Lampe, Phys. Fluids 23, 2383 (1980).

33. B. Rossi and K. Greisen, Rev. Mod. Phys. 13, 240 (1941).

34. G. Moliere, Z. Naturforsch A3, 78 (1948).

35. E. J. Williams, Proc. R. Soc. London Ser. A 169, 531 (1939).

36. H. A. Bethe, Phys. Rev. 89, 1256 (1953).

37. W. H. Bennett, Phys. Rev. 45, 890 (1933).

38. W. H. Bennett, Phys. Rev. 98, 1584 (1955).

PART C

IBEX Beam Hollowing Simulations

Brendan B. Godfrey

Mission Research Corporation
Albuquerque, New Mexico 87106

and

Carl A. Ekdahl

Sandia National Laboratories
Albuquerque, New Mexico 87185

I. INTRODUCTION

The resistive hollowing instability has long been considered a critical issue for high current electron beam transport in air. The instability occurs routinely in computer simulations for beam currents above 17 kA and risetimes less than a few ns in full density air, and over broader parameter ranges at reduced air densities.[1-6] It develops rapidly in the beam nose and is highly disruptive. Although emittance tailoring and electron energy spread can raise the threshold for the onset of hollowing,[4] the stability of high current beams against hollowing can be assured only by maintaining a sufficiently long current risetime.[3,7] More background is provided in Part B.

A series of three high current beam experiments have been performed to confirm this theoretical picture of the hollowing instability. Beam hollowing was proven to exist in research by C. Ekdahl and W. Bostick, carried out at densities of about 1 Torr with the Air Force Weapons Laboratory 1.5 MeV, 40 kA FX-100 beam.[8] Attempts to simulate this behavior numerically were unsuccessful, probably because available air chemistry models were inadequate at such low pressures and because the instability occurred late in the pulse. Subsequently, R. Adler, G. Kiuttu, and B. Sabol extended the hollowing observations up to 20 Torr in air using the Air Force Weapons Laboratory 1.1 MeV, 20 kA VISHNU accelerator.[9] Simulations achieved qualitative agreement with experiment, exhibiting severe hollowing near the beam nose, which eroded rapidly, over the pressure range in question. (A nondisruptive hollowing, which is not well understood, but appears to be associated with very high plasma return current fractions and long decay times, often arose later in the pulse.) In both experiments and simulations, hollowing instability frequencies were effectively zero, consistent with the fact that measured return current decay times were comparable to the beam pulse lengths.

Theory predicts that the hollowing instability threshold scales as the time derivative of the beam current divided by the air density, and that for a give beam current waveform the instability does not occur above a specified

pressure. This stability threshold is a sensitive measure of the accuracy of our theoretical models. For this reason C. Ekdahl and coworkers undertook a third experiment on the Sandia National Laboratories 4 MeV, 70 kA, 15 ns rise-time IBEX accelerator. Hollowing, sometimes followed by filamentation, was observed throughout the 10-80 Torr air density range.[10] The amplitude of the hollowing decreased sufficiently fast at the higher densities that it was possible to extrapolate a cutoff at 100-120 Torr, which is consistent with theoretical predictions if nose erosion and finite drift tube length are taken into account.[7] The instability frequencies were again vanishingly small, and the wavelengths were 50 - 100 cm. Typically, 17 kA net (i.e., beam plus plasma) currents and 100 ns plasma current decay times were measured.

We report here a comprehensive set of axisymmetric simulations performed to aid in interpreting the IBEX experimental results. Agreement between simulation and experiment was surprisingly good. The similarity between open shutter photographs of the unstable beam and computer-generated beam distributions is particularly striking. The simulations yielded three principal results. First, an instability threshold of 120-140 Torr was obtained. Second, the beam was least unstable to hollowing when the radius at injection equaled its matched radius in air. Third, eliminating the low energy electrons which occur naturally at the head of a diode-generated beam reduces the hollowing threshold to about 80 Torr. The combination of experiments, simulations, and emperical scaling relations give us confidence that the hollowing instability will not prevent high current beam transport in uniform density air.

Part C is divided into seven sections. Section II summarizes present theoretical understanding of the hollowing instability as it applies to the IBEX experiments. The experimental results are summarized in Sec. III. Sections IV, V, and VI then elaborate on the principal simulation findings enumerated above. We briefly state our conclusions in Sec. VII. Nonaxisymmetric studies, now in progress, will be reported at a later date.

II. INSTABILITY SCALING RELATION

It is clear from simulations that the hollowing instability is associated with conductivity and return current radial profiles which are strongly peaked on axis. A comprehensive study by G. Joyce and colleagues at the Naval Research Laboratory indicates that secondary electron avalanche in the beam head is central to triggering disruptive hollowing, which occurs for the ratio of peak inductive electric field to air density,[3]

$$E/P > 130 \text{ kV/cm-Atm.}$$

In addition, the net current must be less than half the beam current, although this criterion usually is met whenever the E/P requirement is satisfied. These conditions were developed primarily from 10 kA beam simulations. Our own studies for high current beams for the most part yield similar results,[4] even for initially annular profiles.[11]

In Part B of this report we converted the E/P criterion to an $\dot{I}/P$ threshold curve for various densities, where $\dot{I}$ is the current riserate. This threshold, as applied to the IBEX beam, is shown in Fig. 1. Also depicted is the parameter regime accessible to IBEX. The instability threshold can, in principle, be observed experimentally and compared with theory by varying the air density from shot to shot and measuring the hollowing amplitude. In practice, nose erosion and limited propagation length complicate such a comparison, making parallel simulations desirable.

Theory predicts as well that the hollowing instability frequency, ω, scales as the inverse of the monopole decay time, and the Doppler-shifted frequency, ω-kv, scales as the betatron frequency.[4,7]

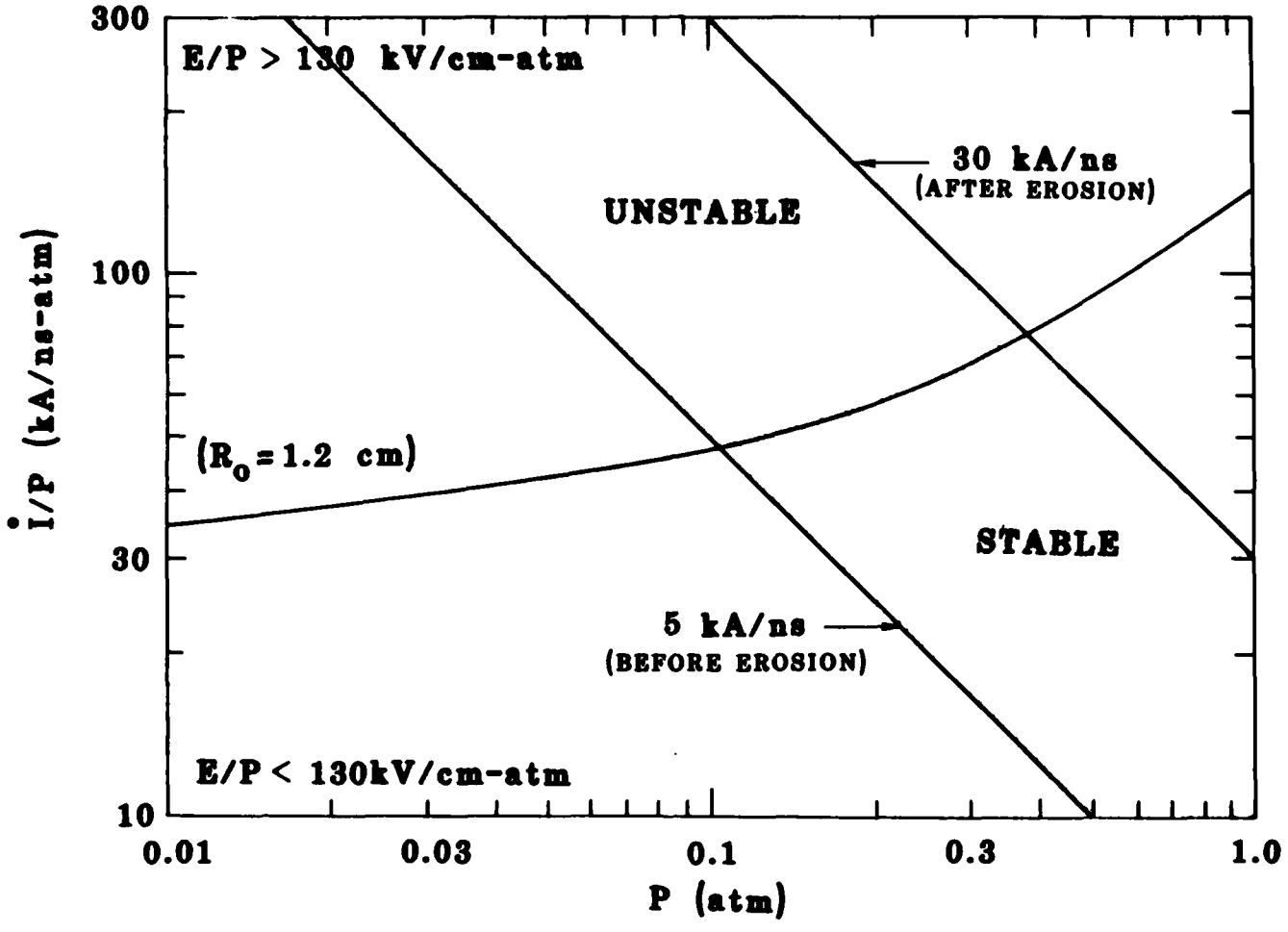

Figure 1. Operating regime of IBEX hollowing instability experiment. Indicated are the instability threshold beam current riserate (solid curve) and the experimentally accessible range of riserates (shaded area).

III. EXPERIMENT SYNOPSIS

The IBEX accelerator current and voltage waveforms were approximately trapazoidal with a 15 ns risetime and a 5 ns flattop. Peak current and voltage were 70 kA and 4 MeV, respectively. In this experiment the beam at injection was measured to have roughly a Bennett radial profile with a half radius of order 1.0 cm. The metallic drift chamber was 20 cm in radius and 150 cm in length, it windows shielded with screen. Open-shutter optical photography, x-ray framing camera photography, and segmented Faraday cups were available in addition to the usual current and voltage diagnostics.

Competition from the hose instability has always been a major problem in observing the hollowing instability. Here, the hose threshold was pushed to 80 Torr by an emperically determined optimal anode foil, 305 μm (12 mil) Ti. The corresponding RMS scattering angle at 4 MeV, determined using the CYLTRAN Monte Carlo electron-photon transport code,[12] is 20°,[13] which leads to a matched emittance for the 17 kA net current. Matching occurs for a Bennett profile beam[14],[15] when

$$\langle\theta^2\rangle \approx \nu_n/\gamma$$

where θ is the scattering angle, ν_n is the net current normalized to 17 kA, and γ is the electron relativistic energy.

The hollowing instability was observed throughout the pressure range 10-80 Torr. At the lower pressures the instability was long wavelength and large amplitude, while at 80 Torr it was unobservable without careful examination of end-on x-ray framing camera images. (In fact, the reevaluation of this data which uncovered hollowing at 80 Torr was prompted by the observation of weak hollowing in simulations.) An extrapolation of the hollowing instability amplitude variation suggests a threshold at 100 to 120 Torr. In all cases the instability frequency was vanishingly small. The measured return current decay time was between 80 and 110 ns.

Subsequent filamentation of the hollowed beam often was observed at the lower pressures. Azimuthal modes 3 to 6 dominated.[10]

IV. EFFECTS OF AIR DENSITY VARIATION

Computer simulations were for the most part performed in the laboratory frame using the CPROP particle-in-cell code[2] with Moliere scattering[16-18] and BMCOND air chemistry.[19] Experimental initial conditions were modeled as closely as possible. Thus, the current and voltage were ramped linearly over 15 ns to their peak values and then held constant for from 5 to 8 ns. A 1.2 cm radius Bennett profile truncated at about 4 cm was employed. Electron transverse velocities were initialized from a Gaussian distribution in sin θ such that

$$\gamma \langle \sin^2\theta \rangle^{1/2} = 3.1,$$

which approximates the effect of the 305 μm Ti foil on an otherwise cold beam. The cylindrical computational mesh was 150 cm in length, 20 cm in radius, and bounded by conducting walls, just as in the experiment. Zoning was exponential in radius.

Computations were carried out at 40, 80, 120, and 160 Torr. As expected, erosion was very rapid, varying from 0.4 to 0.5 with increasing air density. The beam current riserate, therefore, increased from 5 kA/ns at the drift tube entrance to roughly 50 kA/ns at the exit. The rapid current rise was due in part to axial bunching of low energy beam electrons. Because observed instability growth is determined by beam properties in the central portion of the drift tube, an eroded beam riserate of 30 kA/ns is appropriate for comparison with theory. Typical peak electric field strengths ranged from 40 to 70 kV/cm, again increasing with air density. Average net currents (at peak beam current) were within 10% of 17 kA, which agrees well with experiment. Monopole decay times in the simulations were of order 35 ns. Multiplying by the beam-cavity inductance factor, here about 3, gives the experimentally measured return current decay time.

Large amplitude, low frequency hollowing developed early in the 40 Torr runs and persisted throughout the beam pulse. Figure 2 is a typical r-z plot. Such figures are quantitatively similar to open shutter photographs from the

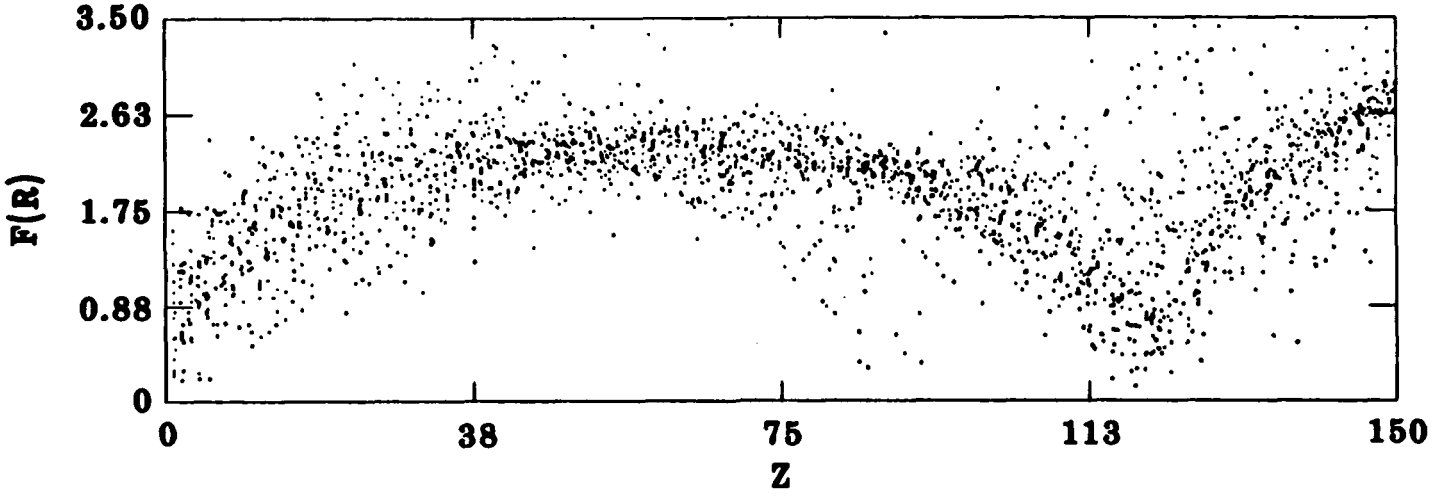

Figure 2. R-Z particle plot 20 ns into a 40 Torr simulation. Well defined, large amplitude hollowing is evident. (The radial dimension is scaled exponentially.)

experiment.[10] Numerically generated x-ray photographs at the endplate also resemble corresponding experimental data, in this case a sharply defined annulus of 12 cm radius and 2 cm thickness. Note, though, that quantitative features of the x-ray photographs depend sensitively on the phase of the wave pattern at the endplate and so do not necessarily provide a reliable measure of the instability amplitude.

The hollowing instability at 80 Torr was somewhat smaller in amplitude and shorter in wavelength, as shown in Fig. 3. The corresponding numerical x-ray photograph indicates a 5 cm radius annulus, less well defined than for the 40 Torr runs. At 120 Torr, outside the pressure range of the experiments, the simulated IBEX beam was hollowing unstable only in the nose, and at later times the instability died away. This transient hollowing would not have been observable with diagnostics available on the experiment. A 160 Torr simulation showed no sign of hollowing whatsoever. On this basis, the hollowing instability threshold for the simulations lies in the range 120-140 Torr.

The instability threshold from Fig. 1 is much higher, approximately 350 Torr. The difference arises from the finite length of the drift tube. There was simply not enough propagation distance for the instability to develop at the higher pressures. Nonetheless, because the agreement between simulation and experiment is so good, and the curve in Fig. 1 was based on such simulations over longer distances, we may conclude that the experiments confirm our understanding of the hollowing instability.

V. EFFECTS OF EMITTANCE MISMATCH

A 305 μm Ti anode foil proved to give the most stable beam behavior experimentally. For a 17 kA net current the scattering imparted by this foil leads to a matched beam at injection. Different initial scattering angles, both larger and smaller than the 305 μm Ti value, were simulated for 80 Torr air. As in the experiment, the 20° scattering resulted in least hollowing. Presumably, a matched beam is best because initial perturbations which may trigger instabilities are smallest. Hot spots of high conductivity due to periodic pinching of a mismatched beam also are avoided.

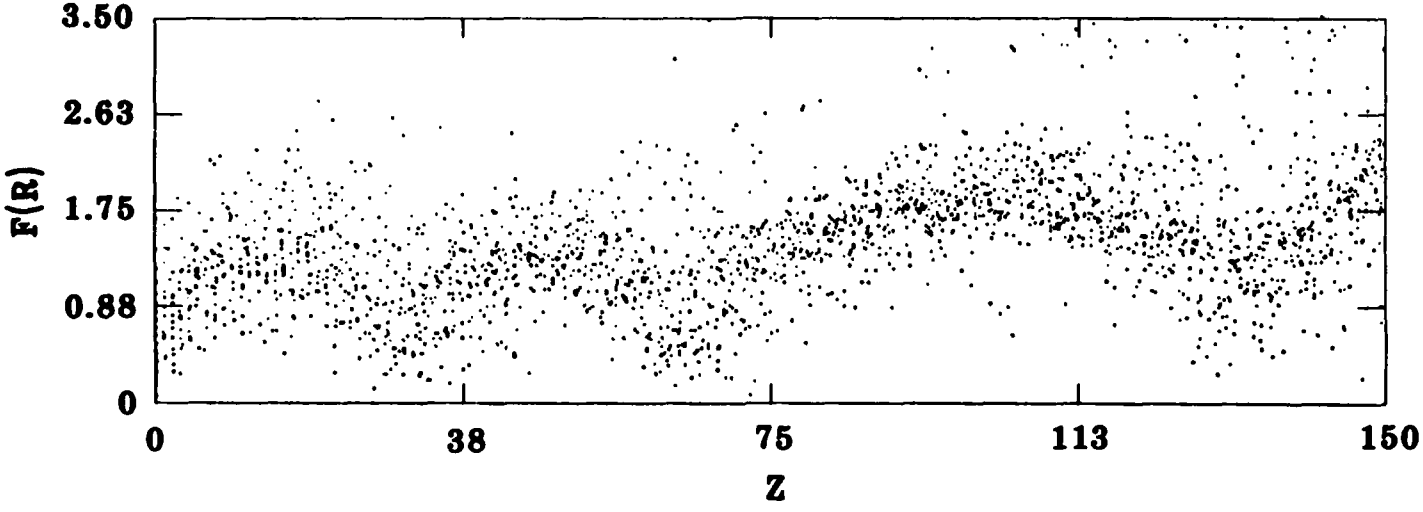

Figure 3. R-Z particle plot 20 ns into an 80 Torr simulation. Small amplitude, low frequency hollowing is evident. (The radial dimension is scaled exponentially.)

Beam pinching in the diode also might cause a mismatch, a possibility suggested by S. Putnam.[20] Since time did not permit determining the beam convergence experimentally, it was necessary to estimate this behavior computationally. Diode simulations by D. Pershing and colleagues[21] and by J. Quintenz[22] predicted a maximum pinch angle at the anode foil of about 18°, while at the same time reproducing the experimentally measured beam current. Note, however, that the current density radial profile was less well represented. Figure 4 depicts typical particle trajectories and potential contours generated by the SCRIBE code[21] for the 4 MeV IBEX diode. Calculations were performed at lower voltages as well. These results were synthesized into a radially and temporally varying model of the beam convergence angle at the drift tube entrance foil,

$$\theta = (r/a)\{(0.524 - 0.140(r/a))T - 0.105\}$$

Here, T increases linearly from zero to one during the current rise; a is the Bennett radius.

Diode pinching had minimal effect in the 40 Torr simulations. At 80 Torr, however, hollowing was enhanced noticeably, and the instability wavelength was reduced slightly. Moreover, a weak instability persisted at 120 Torr even at late times. The beam remained stable at 160 Torr. The overall impact of beam convergence in the diode, therefore, was to raise the instability threshold by roughly 20 Torr.

Consistent with the supposition that beam pinching in the diode enhances hollowing only through an emittance mismatch, one would expect the effects of pinching to become negligible for maximum pinch angles much less than the mean foil scatter angle. An 80 Torr simulation with the maximum convergence angle halved to 9° confirmed this expectation.

VI. EFFECTS OF LOW ENERGY ELECTRONS

As noted above, low energy beam electrons injected during the rising portion of the diode voltage contributed significantly to a rapid sharpening of the beam nose both by bunching axially and by enhancing erosion. Axial bunching, in particular, is more severe when electrons are born at low energies than

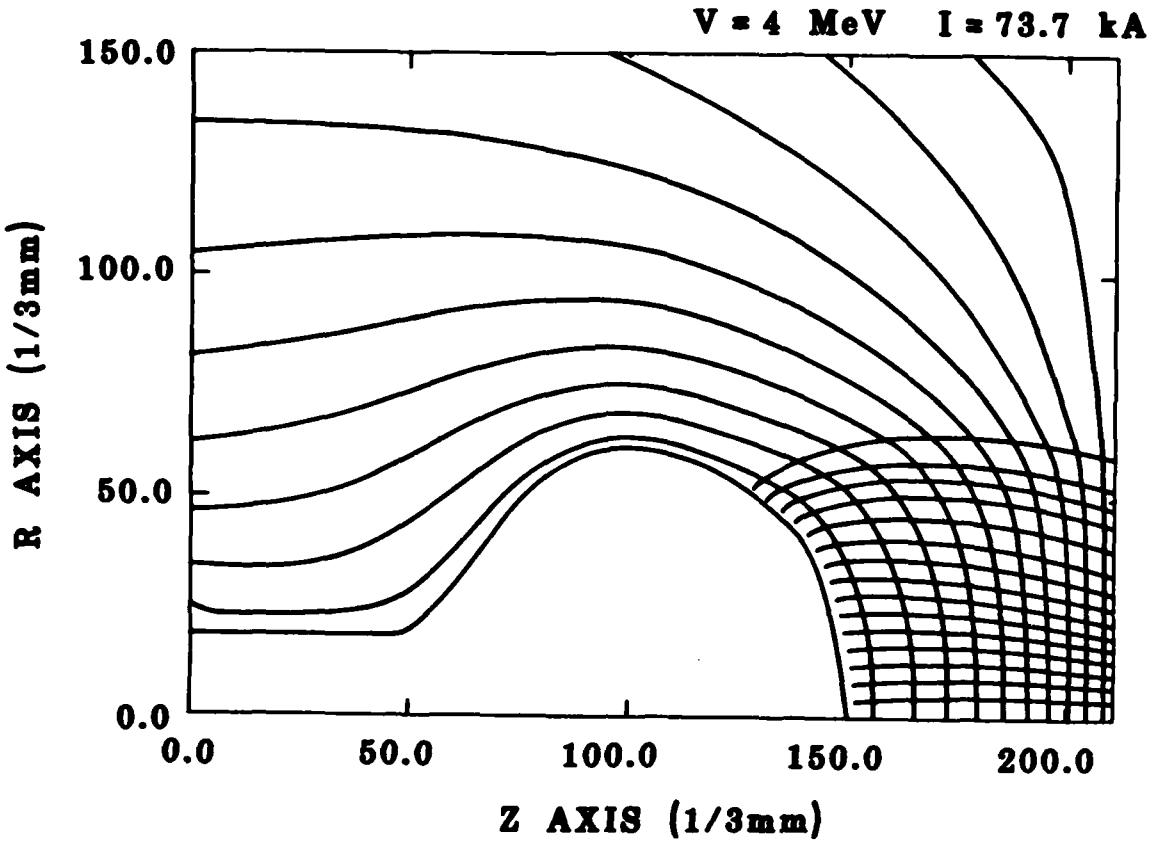

Figure 4. Representative electron trajectories and equipotential lines from a SCRIBE calculation of the IBEX diode.

when originally high energy beam electrons lose energy inductively at the beam head. In the latter case the electrons are scattered by the air to large radii as they slow down, while in the former there is little time for the scattering to have effect. (Nonetheless, omitting air scattering significantly increased the degree of hollowing in 40 and 80 Torr simulations.)

A single 80 Torr run without a beam energy ramp substantiated these observations. The erosion rate dropped to 0.3, no axial bunching occurred, and the current riserate did not increase above 10 kA/ns. Most importantly, peak electric fields in the central portion of the drift tube averaged about 15 kV/cm, and only a weak, nondisruptive hollowing instability developed. Hollowing was localized to near the axis, reminiscent of late time behavior in VISHNU beam simulations.[4,9] See Fig. 5.

A voltage ramp is characteristic of diode-generated beams. Conditioning to remove the low energy particles should reduce the likelihood of a hollowing instability, at least over short propagation distances. It also may have a salutory influence on other resistive instabilities. We remark that extracting an electron beam from a magnetic-field-immersed diode tends to strip off low energy electrons.[23] Evidence exists that the VISHNU[9] and IBEX[24] beams were less subject to the hose instability when extracted from immersed diodes. High energy beams from multi-stage accelerators, such as RADLAC at Sandia National Laboratories[25] and ATA at Lawrence Livermore National Laboratory,[26] should have minimal energy ramps.

VII. CONCLUSIONS

The good agreement achieved between IBEX experiments and simulations presented here confirms our ability to predict the stability of high current electron beams in uniform density air against hollowing. The code results also emphasize the need to avoid emittance mismatches and voltage ramps when injecting beams into air. Similar simulations in Part B of this report predict no hollowing over a Nordsieck length for a beam of sufficiently slow initial risetime. We look forward to RADLAC and ATA beam experiments confirming our optimism.

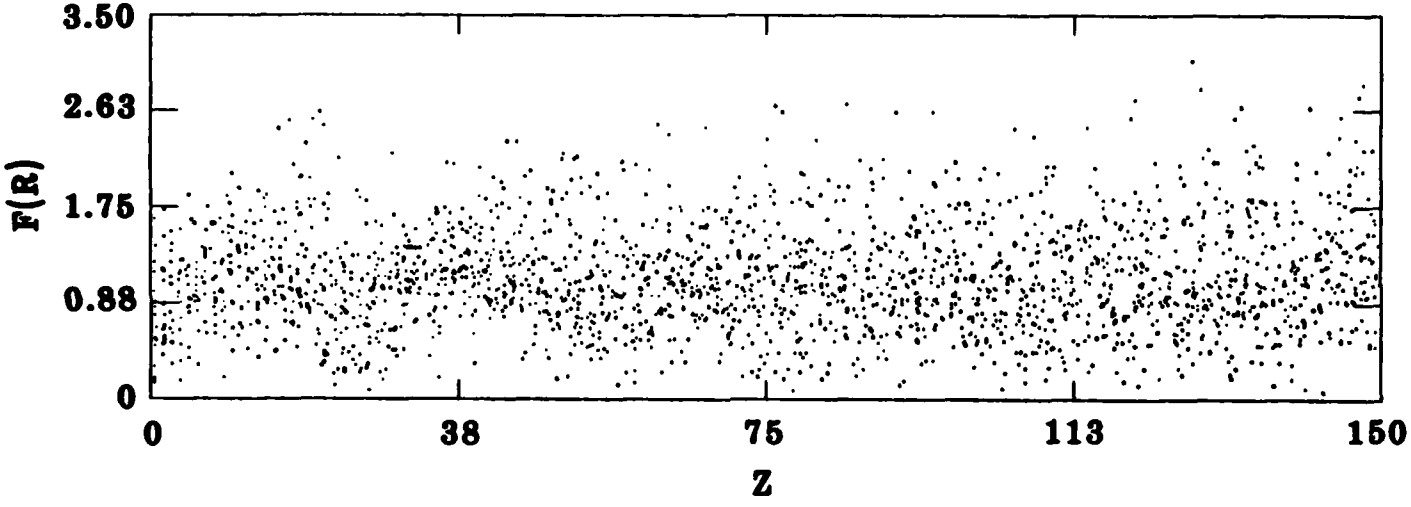

Figure 5. R-Z particle plot 20 ns into an 80 Torr simulation with the beam energy ramp omitted. Hollowing is minor. (The radial dimension is scaled exponentially.)

ACKNOWLEDGEMENTS

It is a pleasure to recognize the contributions of J. Freeman, J. Quintenz, S. Putnam, D. Pershing, C. Sedlak, R. Jackson, and M. Campbell to this investigation.

The study was supported by the Sandia National Laboratories, Albuquerque, by the Air Force Weapons Laboratory, and by the Defense Advanced Research Projects Agency (contract monitored by the Naval Surface Weapons Center, White Oak).

REFERENCES

1. F. W. Chambers, "Sausage Mode Stability Boundaries: Enumeration and Verification," UCID-18879 (Lawrence Livermore National Laboratory, Livermore, 1980).

2. B. B. Godfrey, "High Current Beam Propagation Study," AMRC-R-367 (Mission Research Corporation, Albuquerque, 1982).

3. G. Joyce and M. Lampe, Phys. Fluids 26, 3377 (1983).

4. R. R. Johnston, D. A. Keeley, C. L. Yee, B. B. Godfrey, L. Wright, T. Hughes, and N. Carron, "Charged Particle Beam Propagation Studies," SAI-C-57-PA (Science Applications Inc., Palo Alto, 1983) (S/NSI).

5. G. Joyce, M. Lampe, R. R. Hubbard, and R. Fernsler, in High Power Electron and Ion Beams (R. J. Briggs and A. J. Toepfer, Eds.), p. 382 (San Francisco, 1983).

6. K. A. Brueckner, private communication (1983).

7. B. B. Godfrey, R. J. Adler, M. M. Campbell, N. J. Carron, T. P. Hughes, G. F. Kiuttu, N. F. Roderick, and L. A. Wright, "Presentation to DARPA/Services Propagation Review," AMRC-N-232 (Mission Research Corporation, Albuquerque, 1983).

8. C. A. Ekdahl, "Beam Propagation Experimental Study," AMRC-R-352 (Mission Research Corporation, Albuquerque, 1982).

9. R. J. Adler, G. F. Kiuttu, B. A. Sabol, W. Bostick, C. A. Ekdahl, L. A. Wright, B. B. Godfrey, T. P. Hughes, N. F. Roderick, and D. J. Sullivan, "Beam Propagation Experimental Study," AMRC-R-466 (Mission Research Corporation, Albuquerque, 1983).

10. C. A. Ekdahl, J. R. Freeman, G. T. Leifeste, R. B. Miller, W. B. Styger, and B. B. Godfrey, submitted to Phys. Rev. Lett. (1985).

11. N. F. Roderick, "Axisymmetric Hollowing Instability in Rotating Annular Beams," AMRC-R-622 (Mission Research Corporation, Albuquerque, 1985).

12. J. A. Halbleib and W. H. Vandeveder, "CYLTRAN: A Cylindrical Geometry Multimaterial Electron/Photon Monte Carlo Transport Code," SAND74-0030 (Sandia National Laboratories, Albuquerque, 1974).

13. J. R. Freeman, private communication (1984).

14. W. H. Bennett, Phys. Rev. 45, 890 (1933).

15. W. H. Bennett, Phys. Rev. 98, 1584 (1955).

16. G. Moliere, Z. Naturforsch A3, 78 (1948).

17. H. A. Bethe, Phys. Rev. 89, 1256 (1953).

18. T. P. Hughes and B. B. Godfrey, Phys. Fluids 27, 1531 (1984).

19. R. L. Feinstein, "BMCOND Model," SAI-U-080-8203 (Science Applications Incorporated, Palo Alto, 1982).

20. S. Putnam, private communication (1984).

21. D. E. Pershing, C. A. Sedlak, R. H. Jackson, M. M. Campbell, and B. B. Godfrey, "Simulation of the IBEX Diode with SCRIBE," MRC/WDC-R-082 (Mission Research Corporation, Washington, 1984).

22. J. Quintenz, private communication (1984).

23. T. P. Hughes and M. M. Campbell, unpublished (1983).

24. R. J. Adler, G. F. Kiuttu, and R. J. Richter-Sand, "Stabilization of the Resistive Hose Instability in Intense Electron Beams," AMRC-R-598 (Mission Research Corporation, Albuquerque, 1984).

25. R. B. Miller, unpublished (1984).

26. G. J. Caporaso, W. A. Barletta, D. L. Birx, R. J. Briggs, Y. P. Chong, A. G. Cole, T. J. Fessenden, R. E. Hester, E. J. Lauer, V. K. Neil, A.C. Paul, D. S. Prono, and K. W. Struve, in Beams '83: High-Power Particle Beams (R. J. Briggs and A. J. Toeffer, Eds.), p. 427 (San Francisco, 1983).

END

FILMED

4-85

DTIC